15 August 1994

PHYSICS LETTERS A

ELSEVIER

Physics Letters A 191 (1994) 201–207

A two-photon interference experiment using type II optical parametric down conversion

Y.H. Shih, A.V. Sergienko

Department of Physics, University of Maryland Baltimore County, Baltimore, MD 21228, USA

Received 28 April 1994; accepted for publication 9 June 1994
Communicated by J.P. Vigier

Abstract

A pair of orthogonally polarized light quanta, produced from type II parametric down conversion, is injected into a single input port of a beamsplitter and detected coincidently by two detectors placed in the two output ports of the beamsplitter. With the help of a set of crystal quartz plates, a Pockel's cell and two linear polarizers, the coincidence counting rate exhibits interference modulation of the pump frequency with 88% visibility when manipulating the voltage across the Pockel's cell, regardless of the optical delay (which is much greater than the coherence length) and the mutual incoherence. This two-photon interference effect is responsible by a nonclassical two-photon state which is entangled *both* in spin and in space–time.

The quantum nature of light produced in spontaneous optical parametric down conversion (OPDC) [1] has received a great deal of attention recently. In OPDC a pair of light quanta is generated simultaneously. The state of the pair, which has been called a two-particle entangled state, cannot be written as products of single photon states [2]. One of the striking consequences of these two-particle entangled states, which was brought to attention by Einstein, Podolsky, and Rosen in the early days of quantum theory [3], is that the measurement of an observable of either particle determines the value of that observable for the other particle with unit probability. The entanglement of the two-particle system could be in spin or in space–time. The measurement of spin variable entanglement started from the early 1950's [4]. It has been understood that the EPR paradox and Bell's inequality [5] violations in these two-particle spin correlation experiments are responsible by a spin variable two-particle entangled state. It has also been realized that the "unusual" two-photon interference phenomena (or fourth order interference phenomena) [6–14] (in Ref. [10] two pioneer experiments with interference visibilities less than 50% were discussed (the coincidence time windows are not narrow enough to "cut off" the long–short and short–long amplitudes)) was also responsible by a space–time variable two-particle entangled state [15].

Spontaneous optical parametric down conversion is an efficient mechanism to produce these two-particle entangled states. In OPDC, a pump laser beam is incident on a birefringent crystal. A pair of photons is generated by the pump in the crystal due to the nonlinear optical effect. The well-known phase matching condition [1] leads to the entanglement of the two-photon state,

$$\omega_1+\omega_2=\omega_p, \qquad \boldsymbol{k}_1+\boldsymbol{k}_2=\boldsymbol{k}_p, \tag{1}$$

where ω and $\boldsymbol{k}$ represent the frequencies and the wave number vectors for signal (1), idler (2) and pump (p)

SSDI 0375-9601(94)000467-4

of the OPDC. The down conversion is named to be type I, if the pair has parallel polarization, or type II, if the pair is polarized orthogonally. Type I OPDC has been used intensively in the two-photon interference experiments (or fourth order interference experiments) to demonstrate nonclassical interference effects [6–14]. For example, consider sending the down conversion photon pair collinearly to a Mach–Zehnder interferometer which has two detectors placed at the two outputs for coincidence photon counting measurement. When the optical path difference of the interferometer is much greater than the coherence length of the down conversion field, the single detectors do not show interference modulation any more, however, the coincidence counting rate still exhibits interference oscillation. Furthermore, it is very interesting to see that the interference visibility could be increased to approach 100%, when the optical delay between the long and short paths of the interferometer is increased to a value which is greater than the coincidence time window of the coincidence detection [6–10]. Essentially, the above measurements are realizing an Einstein–Podolsky–Rosen (EPR) state with space–time entanglement [15],

$$\Psi_{\mathrm{EPR}} = A(L_1, L_2) + A(S_1, S_2)\,, \tag{2}$$

where the two terms correspond to the two-photon probability amplitudes in which both photons travel through either the longer path or the shorter path of the interferometer to trigger detector 1 and detector 2, respectively. The quantum probability amplitudes $A(L_1, S_2)$ and $A(S_1, L_2)$, in which one photon passes the longer path and the other passes the shorter path of the interferometer to trigger detector 1 or detector 2, respectively, have been "cut off" by the coincidence time window. The EPR state (2) does not have a classical counterpart.

Another way to demonstrate EPR state (2) is to send the parallel polarized pair through a balanced Mach–Zehnder interferometer before entering the second unbalanced Mach–Zehnder interferometer. The first interferometer causes the pair to traverse together through either the long or the short path of the second interferometer resulting in the state (2) [11–14].

We wish to report in this paper another type of two-photon interference experiment which realizes a similar EPR state (2) by a different mechanism which takes advantage of the two-photon state of type II OPDC, in which the two-particle is entangled both in spin and in space–time. In this experiment, a pair of orthogonally polarized light quanta generated from type II down conversion is injected collinearly into a single input port of a beamsplitter and a photon counting detector is placed in each of the two output ports of the beamsplitter. When we manipulate the optical delay, Δl, between the orthogonal components of the down converted beam by inserting birefringent quartz plates and a Pockel's cell in the optical path from the down conversion crystal to the beamsplitter, the coincidence rate of the two detectors exhibits a cosine dependence of the pump frequency, $R_c \simeq R_{c0}[1-\cos(\omega_p \Delta l/c)]$, where c is the speed of light. The modulation visibility is about 88% (without any "accidental" subtraction), despite the following: (1) the optical delay is much greater than the coherence length of the down converted beam; (2) the signal and idler beams are mutually incoherent; (3) the single detector counting rates remain constant when Δl is manipulated; (4) this is only a single input beam-splitting type experiment; and (5) unlike either of the two types of experiments mentioned above that there is no need to have a shorter coincidence time window to "cut off" the long-short and the short-long coincidences and there is no need to use any balanced interferometer.

The schematic set up of the experiment is illustrated in Fig. 1. A cw Argon ion laser line of 351.1 nm is used to pump an 8 mm $\times$ 8 mm $\times$ (0.56 $\pm$ 0.05) mm BBO (β-BaB_2O_4) nonlinear crystal. The BBO is cut at a type II phase matching angle to generate a pair of orthogonally polarized signal and idler photons at 702.2 nm wavelength in a single beam. The down converted beam is separated from the pumping beam by a UV grade fused silica dispersion prism and directed by two pinholes with 2 mm diameters. It then passes through a set of crystal quartz plates. The first three quartz plates, which are 2.4 mm in thickness, are oriented in such a way that the o-ray polarization plane of the quartz plates coincides with the e-ray polarization plane of the BBO. Since quartz is a positive crystal and BBO is a negative crystal, the use of these three quartz plates is for the compensation of the optical delay between the o-ray and the e-ray by the BBO. 13 more crystal quartz plates follow these three. The fast axes of these 13 quartz plates are aligned carefully to be oriented at 45° relative to the o-ray and the e-

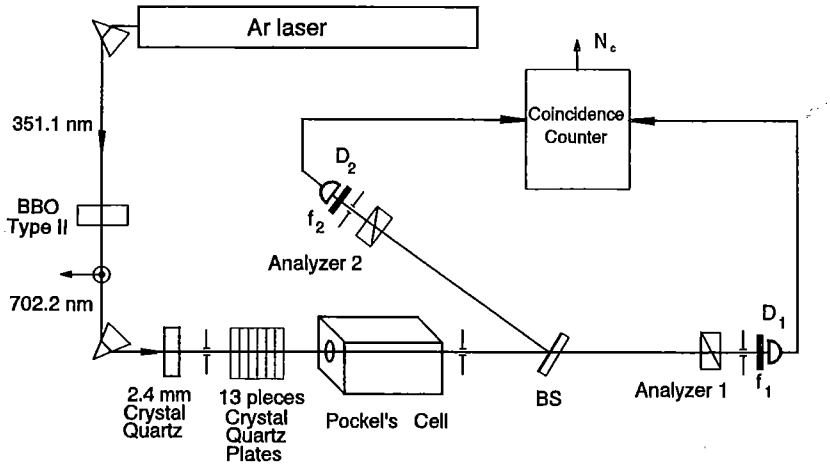

Fig. 1. Schematic experimental set up.

ray polarization planes of the BBO. Each of these quartz plates is (1 ± 0.1) mm in thickness, resulting in an optical delay $\Delta l \simeq 9$ μm between the fast and the slow rays of the quartz crystal at wavelengths around 700 nm. The optical delay is about 117 μm after 13 quartz plates and the coherence length of the field is about 25 μm. Therefore, the $|X\rangle$ and the $|Y\rangle$ components of the o-ray and e-ray of the down conversion suffer enough optical delay to be incoherent, where $|X\rangle$ and $|Y\rangle$ correspond to the fast and the slow axes of the quartz plates. A Pockel's cell with fast and slow axes carefully aligned to match the $|X\rangle$ and the $|Y\rangle$ axes is placed after the quartz plates for fine control of the optical delay between the $|X\rangle$ and the $|Y\rangle$. The quartz plates and the Pockel's cell all have anti-reflection coatings at 702.2 nm. The pair is then injected at a near normal incident angle to a polarization independent beamsplitter which has 50%–50% reflection and transmission coefficients, within ±5% accuracy. A detector package which is composed of a Glan Thompson linear polarization analyzer, a narrow bandwidth interference spectral filter, and a single photon detector is placed in each transmission and reflection output port of the beamsplitter. The photon detectors are dry ice cooled avalanche photodiodes operated in photon counting Geiger mode. The polarization analyzers are oriented at 0° relative to the o-ray polarization planes of the BBO crystal. The spectral filters f_1 and f_2 have Gaussian shape transmission functions centered at 702.2 nm, with bandwidths of 19 nm (full width at half maximum). The output pulses of the detectors are then sent to a coincidence circuit with a 3 ns coincidence time window. In order to have space-like separated detection events the two detectors are separated by about 2 m.

Fig. 2 reports a typical observed interference modulation of the coincidence counting rate as a function of the optical delay Δl_P, where Δl_P is the optical delay (between $|X\rangle$ and $|Y\rangle$) introduced by the Pockel's cell. The manipulation of Δl_P is realized by changing the applied voltage of the Pockel's cell. The half-wave voltage is calibrated at 702.2 nm. The coincidence counts are direct measurements, with no "accidental" subtractions. Each of the data points corresponds to a different voltage applied to the Pockel's cell. The left (right) side data points, which are indicated by a − sign (+ sign), were taken by applying a negative (positive) voltage across the Pockel's cell. It is clear that the modulation period corresponds to the pump wavelength, i.e., 351.1 nm. The interference visibility is about (88 ± 2)%. Contrary to the coincidence counting rate, the single detector counting rate remains constant when Δl_P is manipulated, as is reported in Fig. 2.

The observed phenomenon is a quantum mechanical two-photon interference effect, even though it is only a beam-splitting type experiment. We are going to see that the $\simeq 100$% modulation interference is the result of the nonlocal quantum mechanical superposition of the two-photon probability amplitudes in Eq. (2). The down conversion $|o\rangle$ and $|e\rangle$ polarized photons both have certain probabilities to be in the $|X\rangle$ or the $|Y\rangle$ state when passing through the crystal quartz plates and the Pockel's cell. The optical delay between the $|X\rangle$ and the

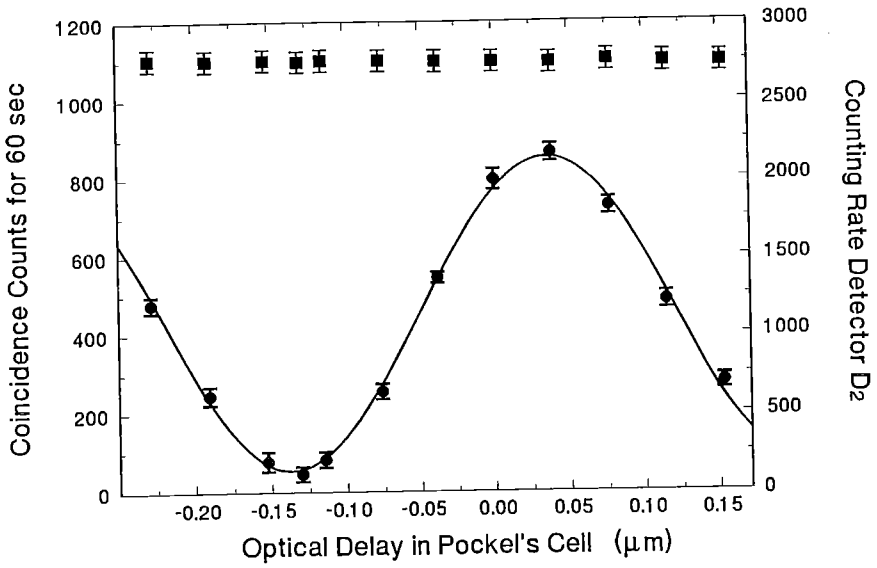

Fig. 2. (Lower part) Coincidence counts in 60 s as a function of the optical delay, Δl_P, which corresponds to a certain voltage applied to the Pockel's cell. (Upper part) Single detector counting rate remains constant when Δl_P is manipulated.

$|Y\rangle$ is then introduced by the anisotropic refractive index of the quartz plates and the Pockel's cell. When the pair meets the beamsplitter, both of the photons have a 50%–50% chance to be transmitted or reflected. The transmitted one is registered by detector 1 and the reflected one is detected by detector 2. It is interesting to see from the following discussion that the only registered coincidences are the two-photon probability amplitudes in which,

(1) ($|o\rangle$ is in $|X\rangle$ and is transmitted)$\otimes$($|e\rangle$ is in $|X\rangle$ and is reflected),
(2) ($|e\rangle$ is in $|X\rangle$ and is transmitted)$\otimes$($|o\rangle$ is in $|X\rangle$ and is reflected),
(3) ($|o\rangle$ is in $|Y\rangle$ and is transmitted)$\otimes$($|e\rangle$ is in $|Y\rangle$ and is reflected),
(4) ($|e\rangle$ is in $|Y\rangle$ and is transmitted)$\otimes$($|o\rangle$ is in $|Y\rangle$ and is reflected).

All the other possible two-photon probability amplitudes cancel each other, regardless of optical delay (greater than coherence length) and mutual incoherence (signal and idler beams), resulting in an entangled EPR state [2,15], which is realized by the measurement. In the following paragraphs we present a simple quantum mechanical model to explain our experiment.

According to the standard theory of parametric down conversion (first order perturbation theory), the two-photon state of the type II spontaneous optical parametric down conversion can be written as [1]

$$|\Psi\rangle = \int \mathrm{d}\omega_p A(\omega_p) \int \mathrm{d}\omega_1 \, \mathrm{d}\omega_2 \, \delta(\omega_1+\omega_2-\omega_p) \, a_o^\dagger(\omega_1) \, a_e^\dagger(\omega_2)|0\rangle \,, \tag{3}$$

where ω_i represents the frequencies, $i=1,2$, and p, linking signal (1), idler (2), and pump (p). The function $\delta(\omega_1+\omega_2-\omega_p)$ represents perfect frequency phase matching of the down conversion. The subscript indices o and e for the creation operators indicate the ordinary and extraordinary rays of the down conversion. We define the z axis to coincide with the collinear $\boldsymbol{k}_1$ and $\boldsymbol{k}_2$ wave vectors of the down conversion fields, and define the x and y axes to coincide with the o-ray and the e-ray polarization directions of the crystal (right-handed natural coordinate system). $A(\omega_p)$ is a spectral distribution function for the pump field, which is considered to be a Gaussian. It is easy to see from Eq. (3) that the two-photon state is entangled both in spin and in space–time.

The fields at the detectors 1 and 2 are given by

$$E_1^{(+)}(t)=\alpha_t\int d\omega f(\omega)\,[\exp(-i\omega t_{1X})\,(\hat{e}_o\cdot\hat{e}_X)(\hat{e}_X\cdot\hat{e}_1)\,a_o(\omega)+\exp(-i\omega t_{1X})\,(\hat{e}_e\cdot\hat{e}_X)(\hat{e}_X\cdot\hat{e}_1)\,a_e(\omega)$$
$$+\exp(-i\omega t_{1Y})\,(\hat{e}_o\cdot\hat{e}_Y)(\hat{e}_Y\cdot\hat{e}_1)\,a_o(\omega)+\exp(-i\omega t_{1Y})\,(\hat{e}_e\cdot\hat{e}_Y)(\hat{e}_Y\cdot\hat{e}_1)\,a_e(\omega)]\,,$$
$$E_2^{(+)}(t)=\alpha_r\int d\omega f(\omega)\,[\exp(-i\omega t_{2X})\,(\hat{e}_o\cdot\hat{e}_X)(\hat{e}_X\cdot\hat{e}_2)\,a_o(\omega)+\exp(-i\omega t_{2X})\,(\hat{e}_e\cdot\hat{e}_X)(\hat{e}_X\cdot\hat{e}_2)\,a_e(\omega)$$
$$+\exp(-i\omega t_{2Y})\,(\hat{e}_o\cdot\hat{e}_Y)(\hat{e}_Y\cdot\hat{e}_2)\,a_o(\omega)+\exp(-i\omega t_{2Y})\,(\hat{e}_e\cdot\hat{e}_Y)(\hat{e}_Y\cdot\hat{e}_2)\,a_e(\omega)]\,, \tag{4}$$

where $\hat{e}_i$ is in the direction of the ith linear polarization analyzer axis, $a_0(\omega)$ and $a_e(\omega)$ are the destruction operators for the o-ray and the e-ray of BBO, α_t and α_r are the complex transmission and reflection coefficients of the beamsplitter, and $f(\omega)$ is the spectral transmission function of the filters. The t_{iX} and t_{iY} are given by $t_{iX}=t-l_{iX}/c$, $t_{iY}=t-l_{iY}/c$, $i=1, 2$, where $l_{iX,Y}=\int dz\, n_{X,Y}(z)$. X and Y, defined by the fast and slow axes of the quartz plates and the Pockel's cell, indicate the optical paths for the X and Y components of the ith beam, and $n_{X,Y}(z)$ is the refractive index at position z for the X or Y components of the beam. We have approximated $(dn/d\omega)_X-(dn/d\omega)_Y\simeq 0$ for simplifying the calculation. The use of pinholes allows a good one-dimensional approximation.

An effective two-photon wavefunction $\Psi(t_1, t_2)$ can be defined from the correlation function to help understand the physics,

$$\langle\Psi|E_1^{(-)}E_2^{(-)}E_2^{(+)}E_1^{(+)}|\Psi\rangle=|\langle 0|E_2^{(+)}E_1^{(+)}|\Psi\rangle|^2=|\Psi(t_1, t_2)|^2\,. \tag{5}$$

It is straightforward to calculate $\Psi(t_1, t_2)$ from Eqs. (4) and (5),

$$\Psi(t_1, t_2)=\alpha_t\alpha_r[(\hat{e}_o\cdot\hat{e}_X)(\hat{e}_X\cdot\hat{e}_1)(\hat{e}_e\cdot\hat{e}_X)(\hat{e}_X\cdot\hat{e}_2)\,A(t_{1X}, t_{2X})+(\hat{e}_e\cdot\hat{e}_X)(\hat{e}_X\cdot\hat{e}_1)(\hat{e}_o\cdot\hat{e}_X)(\hat{e}_X\cdot\hat{e}_2)\,A(t_{1X}, t_{2X})$$
$$+(\hat{e}_o\cdot\hat{e}_Y)(\hat{e}_Y\cdot\hat{e}_1)(\hat{e}_e\cdot\hat{e}_Y)(\hat{e}_Y\cdot\hat{e}_2)\,A(t_{1Y}, t_{2Y})+(\hat{e}_e\cdot\hat{e}_Y)(\hat{e}_Y\cdot\hat{e}_1)(\hat{e}_o\cdot\hat{e}_Y)(\hat{e}_Y\cdot\hat{e}_2)\,A(t_{1Y}, t_{2Y})$$
$$+(\hat{e}_o\cdot\hat{e}_X)(\hat{e}_X\cdot\hat{e}_1)(\hat{e}_e\cdot\hat{e}_Y)(\hat{e}_Y\cdot\hat{e}_2)\,A(t_{1X}, t_{2Y})+(\hat{e}_e\cdot\hat{e}_X)(\hat{e}_X\cdot\hat{e}_1)(\hat{e}_o\cdot\hat{e}_Y)(\hat{e}_Y\cdot\hat{e}_2)\,A(t_{1X}, t_{2Y})$$
$$+(\hat{e}_o\cdot\hat{e}_Y)(\hat{e}_Y\cdot\hat{e}_1)(\hat{e}_e\cdot\hat{e}_X)(\hat{e}_X\cdot\hat{e}_2)\,A(t_{1Y}, t_{2X})+(\hat{e}_e\cdot\hat{e}_Y)(\hat{e}_Y\cdot\hat{e}_1)(\hat{e}_o\cdot\hat{e}_X)(\hat{e}_X\cdot\hat{e}_2)\,A(t_{1Y}, t_{2X})]\,, \tag{6}$$

where

$$A(t_1, t_2)=A_0\exp[-\tfrac{1}{8}\sigma_p^2(t_1+t_2)^2]\exp[-\tfrac{1}{4}\sigma^2(t_1-t_2)^2]\exp(-i\Omega_1 t_1)\exp(-i\Omega_2 t_2) \tag{7}$$

for Gaussian filters $f_i(\omega)$ with equal bandwidth σ and a Gaussian spectral distribution of the pump field with bandwidth σ_p, and where Ω_i is the ith filter's center frequency which is related to the peak frequency of the pump, Ω_p, by $\Omega_1+\Omega_2=\Omega_p$ (in this experiment $\Omega_1=\Omega_2$) [16]. Considering the phase shift of π due to reflection and the sign of the projections as well as the 45° orientations of the quartz plates and the 0° orientation of the analyzers, it is straightforward to show that the first four terms can be combined into two terms, which correspond to the two-photon probability amplitudes in Eq. (8), where the Y components (of the o or e) take a longer optical path due to the anisotropic refractive index of the quartz plates and the Pockel's cell. It is also straightforward and very interesting to see that other terms in Eq. (6) are *out of phase* in pairs (terms 5–6, and 7–8) and *cancel each other* regardless of optical delay (which is greater than the coherence length) and mutual incoherence (between the signal and idler beams), which has no classical interpretation. The cancellation makes the interference visibility greater than 50%. We want to remind the reader once again that we have used a right-handed natural coordinate system with respect to the $\boldsymbol{k}$ vector as the positive z axis direction. To realize the state of the type in Eq. (2), we have taken advantage of the polarization entanglement of the two-photon state for the cancellation of the unwanted amplitudes. An entangled two-photon state is finally realized by the coincidence measurement,

$$\Psi_{EPR}=A(t_{1X}, t_{2X})-A(t_{1Y}, t_{2Y})\,, \tag{8}$$

which is similar to the EPR state (1), with X and Y equivalent to the long and short paths of the interferometer.

The coincidence counting rate is calculated from,

$$R_c = \frac{1}{T}\int_0^T \int dT_1\, dT_2\, |\Psi(t_1, t_2)|^2\, S(T_1 - T_2, \Delta T_c)\,, \tag{9}$$

where T_i is the detection time of the ith detector, $S(T_1-T_2, \Delta T_c)$ is a function that describes the coincidence circuit, and ΔT_c is the time window of the coincidence circuit. For $|T_1-T_2| > \Delta T_c$, $S(T_1-T_2, \Delta T_c) \simeq 0$, for $|T_1-T_2| < \Delta T_c$, $S(T_1-T_2, \Delta T_c) \simeq 1$. In this experiment the coincidence time window is large enough that we consider $S(T_1-T_2, \Delta T_c) = 1$. The time integral is taken to infinity as a good approximation. The coincidence rate R_c is,

$$R_c = R_{c0}\{1 - \exp[-\sigma_p^2(\Delta l/2c)^2]\cos(\omega_p \Delta l/c)\}\,, \tag{10}$$

which indicates an interference modulation of the pump frequency with 100% visibility when Δl is much smaller then the coherence length of the pump in perfect experimental conditions. The observed visibility is $(88 \pm 2)\%$. The reason we see less than 100% is mainly due to the nonlinear response and the optical quality of our Pockel's cell when applying higher voltages.

We have also demonstrated a similar experiment with an orthogonal circularly polarized light quanta pair. The experimental set up is almost the same except that (see Fig. 3): (1) a quarter-wave plate is placed after the compensation quartz plates. The quarter-wave plate is oriented at 45° relative to the o-ray polarization plane of the BBO to rotate the linear polarization state of the o-ray and the e-ray to an orthogonal circular polarization (left-hand, right-hand) configuration. (2) 13 crystal quartz plates are used to make a large enough delay between $|x\rangle$ and $|y\rangle$ components of the circular polarized pair, where $|x\rangle$ and $|y\rangle$ are defined by the fast and the slow axes of the quartz plates. $|x\rangle$ and $|y\rangle$ are oriented to coincide with the o-ray and the e-ray polarization planes of the BBO. (3) a Pockel's cell is placed after the quartz plates for fine control of the optical delay between $|x\rangle$ and $|y\rangle$. The fast and the slow axes of the Pockel's cell are aligned to match $|x\rangle$ and $|y\rangle$. (4) the polarization analyzers are both oriented at 45° relative to $|x\rangle$. The differences of the two configurations are illustrated in Fig. 3. The coincidence counting rate for the circular configuration exhibits similar interference as that reported in Fig. 2.

In summary, in a simple beam-splitting type experiment we demonstrated a nonclassical two-photon interference phenomenon. A two-photon entangled state is responsible for this "unusual" effect. The two-particle state

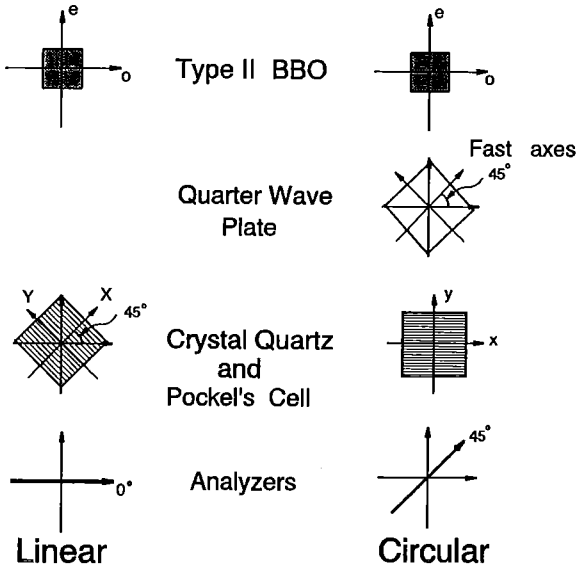

Fig. 3. Experimental set up differences between the linear and circular configuration.

of type II down conversion is entangled *both* in spin and in space–time. This two-photon space–time variable interference experiment has taken advantage of the spin entanglement feature of the state.

We wish to thank M.H. Rubin and D.N. Klyshko for useful discussions. This work is supported by the US Office of Naval Research Grant no. N00014-91-J-1430.

References

[1] D.N. Klyshko, Photons and nonlinear optics (Gordon and Breach, New York, 1988).
[2] E. Schrödinger, Naturwissenschaften 23 (1935) 807, 823, 844 [English translation of these papers appears in Quantum theory and measurement, eds. J.A. Wheeler and W.H. Zurek (Princeton Univ. Press, Princeton, 1983)].
[3] A. Einstein, B. Podolsky and N. Rosen, Phys. Rev. 47 (1935) 777.
[4] C.S. Wu and I. Shaknov, Phys. Rev. 77 (1950) 136.
[5] J.S. Bell, Physics 1 (1964) 195.
[6] J.D. Franson, Phys. Rev. Lett. 62 (1989) 2205.
[7] J. Brendel, E. Mohler and W. Martienssen, Phys. Rev. Lett. 66 (1991) 1142.
[8] P.G. Kwiat, A.M. Steinberg and R.Y. Chiao, Phys. Rev. A 47 (1993) 2472.
[9] Y.H. Shih, A.V. Sergienko and M.H. Rubin, Phys. Rev. A 47 (1993) 1288.
[10] P.G. Kwiat, W.A. Vareka, C.K. Hong, H. Nathel and R.Y. Chiao, Phys. Rev. A 41 (1990) 2910; Z.Y. Ou, X.Y. Zou, L.J. Wang and L. Mandel, Phys. Lett. 65 (1990) 321.
[11] J.G. Rarity and P.R. Tapster, Phys. Rev. Lett. 64 (1990) 2495.
[12] J.G. Rarity, P.R. Tapster, E. Jakeman, T. Larchuk, R.A. Campos, M.C. Teich and B.E.A. Saleh, Phys. Rev. Lett. 65 (1990) 1348.
[13] Z.Y. Ou, X.Y. Zou, L.J. Wang and L. Mandel, Phys. Rev. A 42 (1990) 2957.
[14] T.S. Larchuk, R.A. Campos, J.G. Rarity, P.R. Tapster, E. Jakeman, B.E.A. Saleh and M.C. Teich, Phys. Rev. Lett. 70 (1990) 1603.
[15] M.A. Horne, A. Shimony and A. Zeilinger, Phys. Rev. Lett. 62 (1989) 2209.
[16] Y.H. Shih and A.V. Sergienko, Phys. Lett. A 186 (1994) 29.